Available online at www.sciencedirect.com
ScienceDirect
Energy Procedia 97 (2016) 149 – 155
Energy Procedia

European Geosciences Union General Assembly 2016, EGU
Division Energy, Resources & Environment, ERE

The Effect of Hydro Power on the Optimal Distribution of Wind and Solar Generation Facilities in a Simplified Highly Renewable European Power System

Alexander Kies[a,b,*], Bruno U. Schyska[a,b], Lueder von Bremen[a]

[a] *ForWind, Center for Wind Energy Research, Ammerlaender Heerstr. 118, 26129 Oldenburg, Germany*
[b] *Institute of Physics, University of Oldenburg, Ammerlaender Heerstr. 136, 26129 Oldenburg, Germany*

Abstract

We investigate the optimal distribution of wind and photovoltaic generation facilities in Europe. For this purpose, feed-in data covering Europe for the renewable sources wind, photovoltaics and hydro are used. Together with historical load data and a transmission model, a simplified European power system is simulated. The results show that wind should be placed in countries on the shores of the North-Sea while the picture for PV is complex: A band from Germany to Italy over Switzerland is optimal. Furthermore, we show that hydro power has little influence on the optimal distribution.

Peer-review under responsibility of the organizing committee of the General Assembly of the European Geosciences Union (EGU)
Keywords: Renewable Energy ; Energy System Modelling ; Wind Power ; PV Power ; Hydro Power ; Renewable European Power System

1. Introduction

Shares of renewable generation are on the rise all across Europe. The integration of intermittent renewable generation from wind and photovoltaics (PV) into energy systems poses severe balancing challenges. Several possible solutions to overcome these challenges in a fully renewable European power system were already investigated: Optimising the mix of wind and photovoltaics (PV) [1], [2], [3], the need for storage [4], [5], backup [6], or the reinforcement or extension of the transmission grid [7], [8], amongst others. The cost-optimal distribution of generation facilities for wind/PV was investigated in [9]. We adopt several methods and assumptions from that work [9]: First, we employ the same transmission scheme. Second, we limit our system to wind/PV generation facilities, transmission lines and backup. However, and in contrast, we focus on the impact of hydro power on the optimal distribution. For this purpose, we optimise the spatial distribution with respect to the costs in two scenarios: One without hydro power, where all demand is covered by generation from wind/PV and dispatchable backup and another one with hydro power included, where countries are assigned hydro storage and generation capacities adopted from today's situation.

* Corresponding author
E-mail address: alexander.kies@uni-oldenburg.de

Peer-review under responsibility of the organizing committee of the General Assembly of the European Geosciences Union (EGU)
doi:10.1016/j.egypro.2016.10.043

However, the distribution of hydro power is not optimised alongside wind and PV. Instead, it is assumed that today's hydro situation remains unchanged. This assumption seems reasonable, because European hydro power is already fairly well developed today.

2. Data and methodology

We investigate a simplified pan-European power system consisting of $N = 33$ European countries, which are connected via L inter-country transmission links. Every country has a time series of generation $G_n(t) = G_n^W(t) + G_n^S(t)$ from renewable sources and load $L_n(t)$. To ensure a stable power supply, the mismatch between generation and load needs to be covered by the system at all nodes and times. This is expressed via the nodal balancing equation,

$$G_n(t) - L_n(t) = P_n(t) - B_n(t) + C_n(t). \tag{1}$$

$P_n(t)$ is the injection pattern, which describes the export/import balance of a node, $B_n(t)$ is the backup and $C_n(t)$ is the curtailment. A similar model logic is applied in [10].

2.1. Generation and load data

Ten years (2003-2012) of weather data with a spatial resolution of 7 × 7 km and a hourly temporal resolution are used to model feed-in from the renewable sources wind and photovoltaics. Since MERRA reanalysis [11] only provides hourly wind speeds in 10 m and 50 m height with a spatial resolution of $1/2° \times 2/3°$, the MERRA wind speeds were statistically downscaled to the desired resolution. The statistical downscaling consists of three steps: First, MERRA wind speeds were spatially interpolated to the finer grid. Second, wind speeds were logarithmically extrapolated to 140 m. This was done under the assumption of a logarithmic wind profile with surface roughness lengths provided by COSMO-EU [12]. The logarithmic wind profile is given implicitly by

$$\frac{s(z)}{s(z_0)} = \frac{\log(z/z_r)}{\log(z_0/z_r)}, \tag{2}$$

where $s(h)$ is the wind speed at height h, z is the desired height to be extrapolated to, z_0 is the height for which the wind speed is available and z_r is the surface roughness length. Finally, linear regression coefficients between MERRA reanalysis and COSMO-EU analysis wind speeds were calculated for the year 2012. This means that the relationship between COSMO-EU windspeeds s_c and MERRA wind speeds s_m is assumed to be

$$s_c = \epsilon + b s_m, \tag{3}$$

where ϵ and b are the calculated parameters of the linear regression for a single grid point. After calculation of these coefficients this regression was applied on all investigated years. The power curve of an Enercon E-126 at 140 m hub height with 5% plain losses was used to convert wind speed into produced power for every grid cell.
For PV power simulations, images from Meteosat First Generation (MFG) and Meteosat Second Generation (MSG) satellites were used. Surface irradiances were obtained using the Heliosat method ([13], [14]). The conversion of global horizontal irradiance to irradiation on tilted modules is based on the Klucher model [15]. Module temperatures were computed as

$$T_m = T_a + \sigma I_t, \tag{4}$$

where T_a is the ambient temperature, T_m the module temperature and I_t the irradiance on the inclined surface. σ is a factor that was chosen to be 0.036. The module efficiency $\eta(T_m)$ is then calculated as a function of the module temperature for a given irradiance

$$\eta(T_m) = \eta(25°)\,(1 + aT_m)\,, \tag{5}$$

where a is a device-specific parameter. DC power was converted into AC power using the parameter of a Sunny Mini Central 8000TL converter. The German distribution of capacities for wind and PV in dependency of the available resource (average wind speed / average global horizontal irradiation) was empirically derived and adopted for

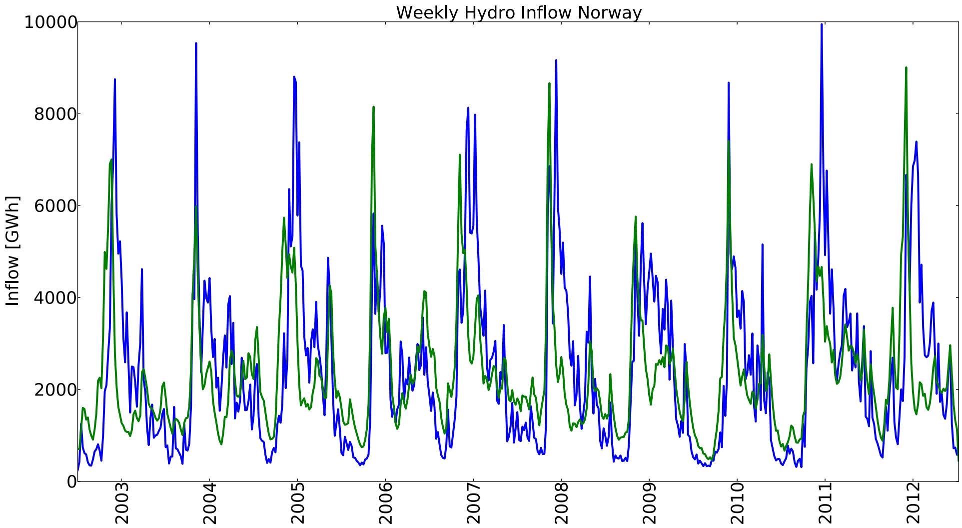

Fig. 1. Weekly measured hydro inflow (green) vs. calculated hydro inflow (blue) for Norway. Source of measured data: Norwegian Water Resources and Energy Directorate

every country. To model hydro power, we chose a potential energy approach using runoff data [16]. The potential gravitational energy of a mass m relative to the sea level is given by

$$U = mgh,$$

where $g = 9.81\mathrm{m/s}^2$ is the constant of gravititational acceleration on Earth and h the height above sea level. Inflow into hydro storages is calculated as a linear function of the potential energy of the runoff

$$I(t) = f \int_A m(t)h(x, y)dA.$$

f is a normalization constant to enforce $\langle \mathrm{I(t)}_n \rangle = \left\langle G(t)_n^H \right\rangle$, where G_n^H is today's average hourly generation from hydro in the corresponding country. Data on today's generation was collected from different sources. The mass is calculated from the runoff data. Measurements are available for Norway and the weekly time series of inflow is shown in Fig. 1. More details on generation data are given in [17]. Load time series have been derived from historical load data provided by ENTSO-E. Load data was modified within the RESTORE 2050 project to account for expected shares from e-mobility and heat pumps and scaled to match scenario B of [18].

2.2. Transmission

To model transmission, we employ the transmission scheme introduced in [9]. If there is an overall negative mismatch $\sum_n (L_n(t) - G_n(t)) < 0$, it is shared among the nodes proportional to their average load,

$$B_n(t) = \max \left\{ 0, \sum_n (L_n(t) - G_n(t)) \right\} \frac{\langle L_n(t) \rangle}{\langle \sum_n L_n(t) \rangle}. \tag{6}$$

The situation is similar, if there is an overall positive mismatch; Curtailment takes place proportional to the average load of the node,

$$C_n(t) = \max \left\{ 0, \sum_n (G_n(t) - L_n(t)) \right\} \frac{\langle L_n(t) \rangle}{\langle \sum_n L_n(t) \rangle}. \tag{7}$$

Consequently, the injection pattern can be calculated from Eq. 1. The flows are connected to the injection pattern via

$$F = K^T L^+ P, \tag{8}$$

where K is the incidence matrix and L^+ the Moore-Penrose pseudoinverse of the Laplacian.

2.3. Quantities of interest

Besides wind and PV (and hydro in one scenario) generation, the investigated system consists of backup and transmission. To minimise the cost, the need for backup energy, backup capacity and transmission capacity are calculated. The need for backup energy is simply given as the temporal integral over the backup events,

$$B_n^E = \int_t B_n(t)dt. \tag{9}$$

To reduce the sensitivity towards the weather database, the 99th quantile of backup and transmission events is used to define the need for backup capacity. Thus, the required backup capacity κ_n^B is calculated according to

$$0.99 = \int_0^{\kappa_n^B} p(B_n)dB_n. \tag{10}$$

Finally, the transmission capacities κ_l^T of the links are calculated,

$$0.99 = \int_0^{\kappa_l^T} p(|F_l|)dF_l. \tag{11}$$

$p(...)$ denote in both cases the distribution of corresponding events.

2.4. Cost assumptions

Predicting the cost development of technical components is a difficult task. Hence, we employ heuristic assumptions to model the costs. For every country the capacity factor for wind onshore, offshore, and PV was computed. The simple assumption is made that each technology has the same financial performance if deployed at its best location on the country level. Stated differently: The cost per GW installed is proportional to the highest capacity factor of this technology among all investigated countries. For backup and transmission cost, the assumption is similarly simple: If the power system is optimised for $\frac{\sum_n \langle G_n(t)\rangle}{\sum_n \langle L_n(t)\rangle} = 1$ (without hydro) with the objective to minimise the need for backup energy, cost for backup energy is equal to 15% of total cost, backup capacity for 10%, and transmission for 10%, as well. Hydro power is assumed to be free of charge.
Summarised, the steps to determine the cost of single components are:

- i) Compute capacity factors for wind onshore/offshore and PV for every country
- ii) Choose highest capacity factor for every technology $\hat{CF}^i$
- iii) Fix cost of technology $i \in \{\text{wind onshore, wind offshore, PV}\}$ as $c^i = CF^i$
- iv) Scale generation of each country such that share of renewables equals one
- v) Calculate cost of generation $\hat{\kappa}$
- vi) Fix cost of backup generation, backup capacity and transmission at $0.15\hat{\kappa}, 0.10\hat{\kappa}$ and $0.10\hat{\kappa}$, respectively.

2.5. Hydro use policy

In the scenario with hydro, the following hydro policy is used: If hydro power is available, it is used to cover the need for power in respect with its constraints. Each country in Europe is assigned a hydro storage capacity $\hat{S}_n^H$, a storage filling level $S_n^H(t)$ and a generation capacity κ_n^H. Aggregated for Europe, hydro storage capacity equals ca. 200 TWh with 190 GW of generation capacity. For every node, renewable generation is extended by generation from hydro,

$$G_n(t) = G_n^W(t) + G_n^S(t) + G_n^H(t), \tag{12}$$

where the generation from hydro is given by

$$G_n^H(t) = \min\left\{S_n^H(t), \kappa_n^H(t), \tilde{G}_n^H(t)\right\} \tag{13}$$

$\tilde{G}_n^H(t)$ is the hypothetical generation,

$$\tilde{G}_n^H(t) = \frac{\langle I_n(t)\rangle}{\sum_n \langle I_n(t)\rangle}\left(-\sum_n \Delta_n(t) + \Lambda(t)\right). \tag{14}$$

where $I_n(t)$ is the time series of energy inflow into hydro reservoirs and $\Lambda(t)$ the constrained generation,

$$\Lambda(t) = \sum_n \left(\tilde{G}_n^H(t) - G_n^H(t)\right). \tag{15}$$

The resulting set of $2N + 1$ equations needs to be solved consistently. The change in storage filling level is then given by

$$S_n^H(t+1) = I_n(t) - G_n^H(t) + S_n^H(t).$$

Initially, all hydro storages are assumed to be empty, i.e. $S_n^H(0) = 0 \forall n$.
Note the following restrictions of the methodology: We aggregated generation and load on the country level. Hence, transmission bottlenecks within single countries were not taken into account. Furthermore, we did not adress frequency stability issues, because the time step of the model is one hour. Third, we chose a heuristic approach to describe the relative costs of system components and therefore do not model them in any way bottom-up.

3. Optimal distribution of wind/PV generation facilities in Europe

The goal of this investigation is to find the distribution of renewable generation capacities leading to the lowest system cost. The system cost is composed of several parts for generation, transmission, and backup,

$$\kappa = \sum_l c^T \kappa_l^T + \sum_n \left(c_C^B \kappa_n^B + c_E^B B_n^E + c^{W/S} C_n^{W/S}\right) \tag{16}$$

where $c_{(..)}^{(..)}$ denote assumed cost and $C_n^{W/S}$ installed capacity for wind/PV. The overall system cost with respect to the capacity distribution C is minimised. Thus, the optimisation problem reads

$$\begin{aligned} &\underset{C}{\text{minimise}}\ \kappa \\ &\text{subject to } C_n^i \geq 0. \end{aligned} \tag{17}$$

First, let us state the main findings of the scenario with hydro included relative to the scenario without hydro:

- The total share of renewables increases in the optimal mix from 0.8 to 0.92
- Total wind onshore capacities installed decrease by 33 GW (5%), wind offshore capacities increase by 7 GW (2%) and PV capacities decrease by 13 GW (3%)
- Cost for backup energy decreases while cost for transmission increases and cost for backup capacity decreases slightly

The optimised distributions of wind and PV capacities are shown in Fig. 2 for both scenarios. Almost no significant changes can be observed. The only striking change is the reduction of PV generation capacities in the Netherlands by ca. 80%, which goes along with increased PV capacities in Southern Europe, especially Italy. Nevertheless, wind onshore/offshore and PV capacities practically remain unchanged overall, while the share of generation rises. However, this rise is entirely caused by the shares of hydro power included in the system. This can be observed in Fig. 3. It shows the system cost in arbitary units according to the chosen heuristic cost assumptions. Overall cost for wind generation (onshore/offshore) is considerably higher than for PV. Cost for backup energy is strongly reduced, which leads to a significant drop of total system cost.

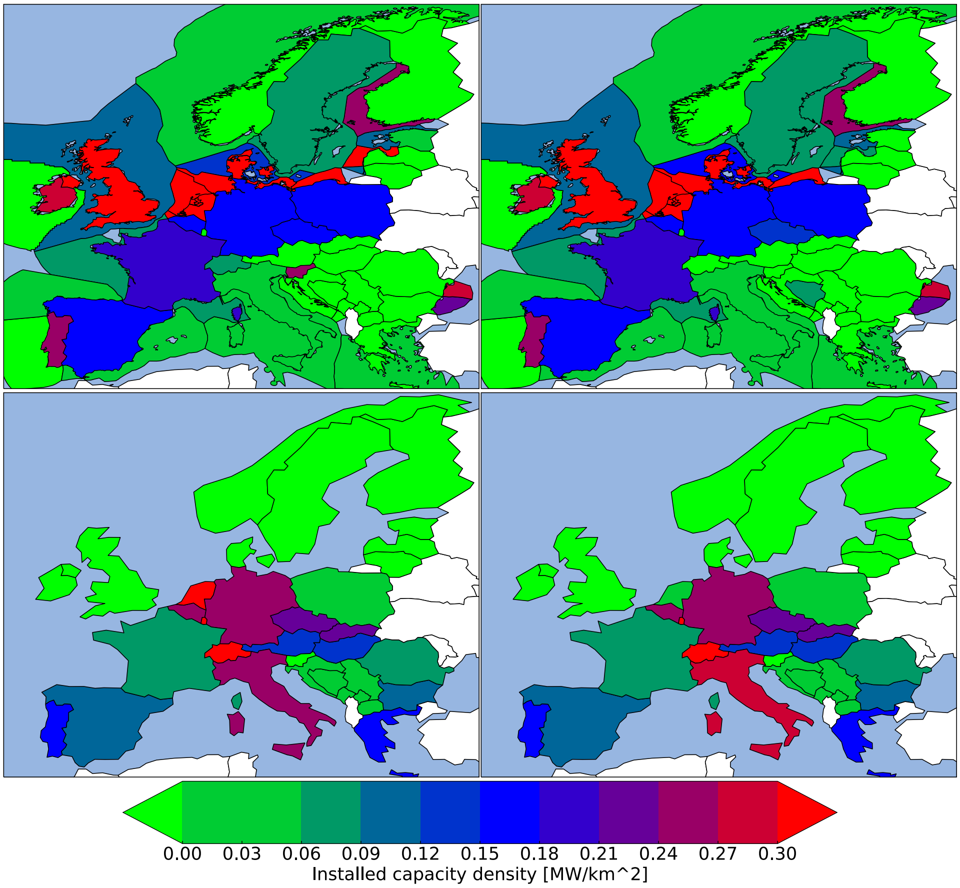

Fig. 2. Optimised distribution of generation capacities without hydro power (left) and with hydro power (right) for wind (top) and PV (bottom).

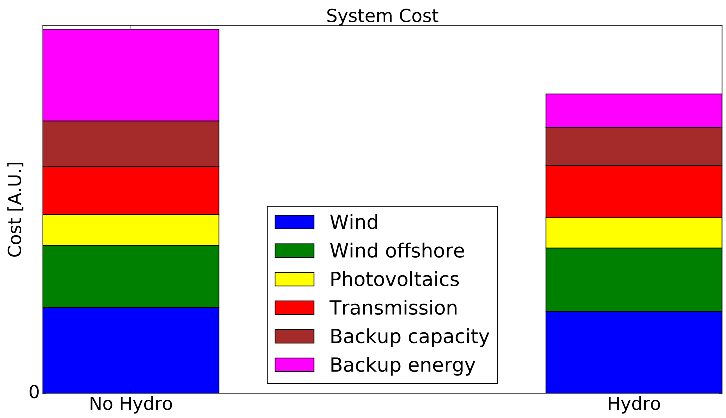

Fig. 3. System cost in arbitrary units with and without hydro.

4. Summary and conclusion

We have optimised the distribution of wind and PV generation facilities in a simplified highly renewable European power system. The simplified system consisted of wind/PV generation facilities, backup and inter-country transmission links. The optimal distribution was found to be: Wind generation in countries on the shores of the North-Sea, PV power in a band from the Netherlands over Germany and Switzerland to Italy. If hydro power is added to the system, the overall distribution patterns do not change significantly. While the overall share of renewables increases due to the hydro power, amounts of wind/PV installed remain the same. Therefore, it can be concluded that hydro power does not have a significant impact on optimised distribution of wind and PV generation facilities in such a simplified European power system. Furthermore, it was found that hydro largely reduces the need for backup energy, but has little effect on the need for backup capacity. This is likely due to the chosen hydro policy. To reduce the need for backup capacity, a different strategy taking the storage filling level into account should be chosen.

Acknowledgements

The work is part of the RESTORE 2050 project (Wuppertal Institute, Next Energy, University of Oldenburg), that is financed by the Federal Ministry of Education and Research (BMBF, Fkz. 03SFF0439A). We thank our project partners for helpful discussions and the provision of load data.

References

[1] Heide, D., Von Bremen, L., Greiner, M., Hoffmann, C., Speckmann, M., Bofinger, S.. Seasonal optimal mix of wind and solar power in a future, highly renewable europe. Renewable Energy 2010;35(11):2483–2489.
[2] Kies, A., Nag, K., von Bremen, L., Lorenz, E., Heinemann, D.. Investigation of balancing effects in long term renewable energy feed-in with respect to the transmission grid. Adv Sci Res 2015;12:91–95.
[3] Lund, H.. Large-scale integration of optimal combinations of pv, wind and wave power into the electricity supply. Renewable Energy 2006;(31):503 – 515.
[4] Weitemeyer, S., Kleinhans, D., Vogt, T., Agert, C.. Integration of renewable energy sources in future power systems: The role of storage. Renewable Energy 2015;(75):14 – 20.
[5] Heide, D., Greiner, M., Von Bremen, L., Hoffmann, C.. Reduced storage and balancing needs in a fully renewable european power system with excess wind and solar power generation. Renewable Energy 2011;36(9):2515–2523.
[6] Huber, M., Dimkova, D., Hamacher, T.. Integration of wind and solar power in europe: Assessment of flexibility requirements. Energy 2014;(69):236 – 246.
[7] Becker, S., Rodriguez, R., Andresen, G., Schramm, S., Greiner, M.. Transmission grid extensions during the build- up of a fully renewable pan-european electricity supply. Energy 2014;(64):404–418.
[8] Kies, A., von Bremen, L., Chattopadhyay, K., Lorenz, E., Heinemann, D.. Backup, storage and transmission estimates of a supra-european electricity grid with high shares of renewables. Proc 14th Wind Integration Workshop 2015;.
[9] Rodriguez, R.A., Becker, S., Greiner, M.. Cost-optimal design of a simplified, highly renewable pan-european electricity system. Energy 2015;83:658–668.
[10] Kies, A., Schyska, B., von Bremen, L.. Curtailment in a highly renewable power system and its effect on capacity factors. Energies 2016;9(7):510.
[11] Rienecker, M.M., Suarez, M.J., Gelaro, R., Todling, R., Bacmeister, J., Liu, E., et al. Merra: Nasa's modern-era retrospective analysis for research and applications. Journal of Climate 2011;24(14):3624–3648.
[12] Schulz, J.P., Schättler, U., Wetterdienst, D.. Kurze beschreibung des lokal-modells europa cosmo-eu (lme) und seiner datenbanken auf dem datenserver des dwd. Tech. Rep.; Deutscher Wetterdienst, Geschäftsbereich Forschung und Entwicklung, Offenbach, Germany; 2011.
[13] Cano, D., Monget, J., Albuisson, M., Guillard, H., Regas, N., Wald, L.. A method for the determination of the global solar radiation from meteorological satellite data. Solar Energy 1986;37(1):31 – 39.
[14] Hammer, A., Heinemann, D., Westerhellweg, A.. Derivation of daylight and solar irradiance data from satellite observations. Proceedings 9th Conference on Satellite Meteorology and Oceanography, Paris; May, 1998, p. 747–750.
[15] Klucher, T.. Evaluation of models to predict insolation on tilted surfaces. Solar Energy 1979;23(2):111–114.
[16] Dee, D., Uppala, S., Simmons, A., Berrisford, P., Poli, P., Kobayashi, S., et al. The era-interim reanalysis: Configuration and performance of the data assimilation system. Quarterly Journal of the Royal Meteorological Society 2011;137(656):553–597.
[17] Kies, A., Chattopadhyay, K., von Bremen, L., Lorenz, E., Heinemann, D.. Restore 2050: Simulation of renewable feed-in for power system studies. Tech. Rep.; University of Oldenburg; 2016.
[18] Pfluger, B., Sensfuß, F., Schubert, G., Leisentritt, J.. Tangible ways towards climate protection in the european union (eu long-term scenarios 2050). Tech. Rep.; Fraunhofer ISI; 2011.